Tangent and Normal Space-Based Method for Dynamics Identification in Microgrids

Hanyang He
Department of Electrical Engineering
The Pennsylvania State University
University Park, Pennsylvania, USA
Email: hfh5310@psu.edu

John Harlim
Department of Mathematics and Meteorology
The Pennsylvania State University
University Park, Pennsylvania, USA
Email: jharlim@psu.edu

Daning Huang
Department of Aerospace Engineering
The Pennsylvania State University
University Park, Pennsylvania, USA
Email: daning@psu.edu

Yan Li
Department of Electrical Engineering
The Pennsylvania State University
University Park, Pennsylvania, USA
Email: yql5925@psu.edu

2024 IEEE Transportation Electrification Conference and Expo (ITEC) | 979-8-3503-1766-4/24/$31.00 ©2024 IEEE | DOI: 10.1109/ITEC60657.2024.10598859

***Abstract*—This paper presents an identification method for the transient dynamics of microgrids that exploits the intrinsic geometric structure of the dynamics, i.e., the high-dimensional states reside on a relatively low-dimensional manifold. In terms of discrete-time dynamics, the increment in states is decomposed into the tangent and normal components using the local geometric information, inferred from the data set of dynamical responses. The sparse identification of nonlinear dynamical systems (SINDy) method and generalized moving least square (GMLS) algorithms are used to estimate the tangent and normal components of increments, respectively, at every time step to constrain the solution onto the manifold of dynamics; this reduces the sensitivity of the SINDy model to candidate function selection and improve the prediction performance. A ten-bus microgrid system with five loads is used to test and verify the effectiveness of the presented method in identifying the system's nonlinear dynamics. Numerical tests show that the developed method can give a better estimation for the dynamic transients caused by load variation, when compared to the traditional SINDy model. The results imply that the proposed method is a useful tool to model the transient dynamics in power systems, especially when the state space lies on a low-dimensional manifold.**

***Index Terms*—System identification, dynamic transients modeling, microgrids, sparse identification of nonlinear dynamical systems (SINDy), generalized moving least square (GMLS)**

I. Introduction

In recent years, the integration of renewable energy sources into power systems has seen significant advancement, largely driven by the global push for sustainable and clean energy. Microgrids, as localized grids that can disconnect from the traditional grid to operate autonomously, play a pivotal role in this transition [1], [2]. However, compared to traditional large-scale systems that have ample inertia, plenty of power electronic devices reduce the inertia of microgrids making them more sensitive to power disturbances caused by load variations. On the other hand, understanding the anti-disturbance capability of microgrids can provide a basis for flexibly scheduling their operation modes. As the transient dynamics identification of microgrids is a key step to solve the challenges mentioned above, it is a meaningful research work to conduct.

When the high-fidelity model is unavailable for the system, it is important to model and predict the system's transients via data. This task is encompassed within the field of system identification (SI). Traditional SI methods can be categorized into two types: linear and nonlinear methods. The linear SI methods include subspace methods [3]–[5], dynamic mode decomposition (DMD) [6], [7], frequency domain analysis and least squares method. These models can effectively identify the locally linearized system with typical functions or structures that is easy to understand and infer the system properties. Also they usually have a lower computational cost. However, it does not accurately identify nonlinear dynamical systems.

Nonlinear SI methods include the Koopman Operator method and neural network-based methods. The Koopman Operator technique transforms nonlinear systems into a linear representation, facilitating analysis, but is limited by computational demands for real-time applications [8], [9]. Also, it is difficult to capture the characteristics of highly nonlinear systems as their eigenvalues are very difficult to obtain. Neural network-based methods leverage the adaptive learning capabilities of neural networks to model complex systems, although they often face challenges with interpretability and overfitting [10], [11]. Additionally, integrating a binary tree algorithm with a nonlinear autoregressive model with exogenous inputs has been explored for modeling nonlinear loads in power systems [12]. However, model building and training can be relatively complex and require specialized technical knowledge.

The sparse identification of nonlinear dynamical systems (SINDy) is a method to discover sparse representable terms embedded the dynamical equations of a system [13]–[15]. It leverages time-evolution data of system states to derive simplified mathematical expressions of system dynamics. Unlike traditional, often inexplicable machine learning methods, SINDy focuses on identifying sparse function structures within dynamics, aiding in uncovering fundamental principles and mechanisms. SINDy is highly versatile and capable of addressing both linear and nonlinear problems by appropriately selecting its candidate function library, making it a popular tool in recent years for addressing SI issues. However, despite its advantages, SINDy faces difficulty in identifying a global model that captures the complete dynamics across the entire data space, especially with limited data. This limitation stems from the method's sensitivity to the choice of candidate function dictionary.

To address this challenge, we impose the local geometric information induced by the data in the SINDy modeling approach. In this case, the negative impact caused by improper selection of candidate functions will be compensated and improved. The key idea is to apply the SINDy method for transient dynamics on a local tangent space induced by the manifold structure encoded in the data, followed by a correction in the normal component via the Generalized Moving Least Square (GMLS) approximation [16] of the exponential map that takes the approximate vector field to the manifold. We will demonstrate the effectiveness of this approach in the identification of microgrid systems.

The content of the paper is listed as follows. The dynamic models of microgrids used to prepare data are introduced in Section II, as well as the problem formulation. Section III gives a detailed introduction to the proposed identification method with geometric constraints. Numerical tests and analysis are given in Section IV. The conclusion is drawn in Section V.

II. Transient Dynamics of Microgrids

In this section, the power system transient model that will be the testbed of the proposed approach is introduced. Particularly, the training and verification data sets will be generated using solutions of this model.

Mathematically, a microgrid system integrated with multiple renewable energy resources can be modeled by using a set of nonlinear differential-algebraic equations (DAEs), as given below.

$$\dot{\mathbf{x}} = \mathbf{f}(\mathbf{x}, \mathbf{y}) \tag{1a}$$

$$\mathbf{0} = \mathbf{g}(\mathbf{x}, \mathbf{y}), \tag{1b}$$

where $\mathbf{x}$ is the state variable, e.g. state variables in the controller of power-electronic interfaces of renewable energy resources; $\mathbf{y}$ is the algebraic variable, e.g., bus voltage amplitude and angle $\mathbf{V}_i = V_i \angle \alpha_i$, and current amplitude and angle $\mathbf{I}_i = I_i \angle \beta_i$; the differential equations $\boldsymbol{f}$ summarize the model of transient dynamics, as explained in the Appendix; algebraic equations $\boldsymbol{g}$ represent the power flow equations that need to be met from the network's perspective.

In practice, building the high-fidelity model that accurately captures the underlying dynamics of a microgrid system is difficult due to incomplete understanding of the physics.

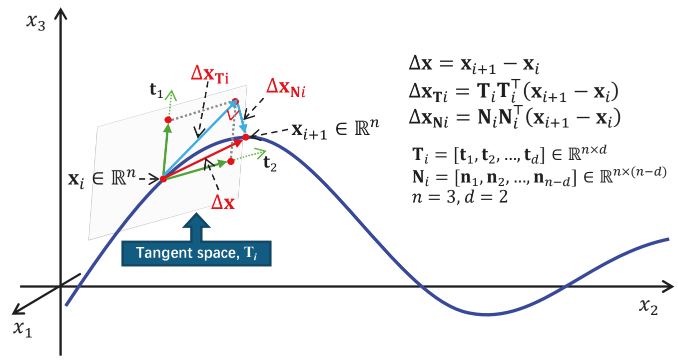

Fig. 1. Illustration of the tangent and normal space-based method.

The goal of this paper is to identify the vector fields of the dynamical system by leveraging the geometric information induced by the algebraic constraints. That is, since the trajectory of the solutions lies on a manifold induced by the algebraic constraints, the vector fields lie on the tangent bundle of the manifold, which naturally motivates an identification leveraging this geometric structure. By leveraging the geometric information, the identified model will become less sensitive to the choice of candidate functions and may perform better with simple polynomial terms.

III. Tangent and Normal Space-Based SINDy Method

A. Overview of the Idea

The core concept of the method is illustrated in Fig.1 for $n = 3$ dimensional state space where the intrinsic manifold is $d = 2$. Define the notation $\mathbf{T}_i$ and $\mathbf{N}_i$ are the tangent and normal space of point i in the state space respectively. Here, we illustrate the increment at each time step of a dynamic trajectory that can be decoupled into two components: the increment in the tangent direction, denoted as $\Delta \mathbf{x}_{\mathbf{T_i}} = \mathbf{T}_i \mathbf{T}_i^\top (\mathbf{x}_{i+1} - \mathbf{x}_i)$, and the increment in the normal direction, denoted as $\Delta \mathbf{x}_{\mathbf{N_i}} = \mathbf{N}_i \mathbf{N}_i^\top (\mathbf{x}_{i+1} - \mathbf{x}_i)$. The increment of the state can be written as,

$$\mathbf{x}_{i+1} - \mathbf{x}_i = \Delta \mathbf{x}_{\mathbf{T_i}} + \Delta \mathbf{x}_{\mathbf{N_i}}.$$

To estimate the rate of change of $\Delta \mathbf{x}_{\mathbf{T_i}}$, a SINDy model with polynomial terms is utilized in this work. Once $\Delta \mathbf{x}_{\mathbf{T_i}}$ is estimated, the increment in the normal direction can then be determined using the GMLS method.

B. Identification in the Tangent Space Increment

The process of model training and parameter preparation is outlined below. In our proposed method, acquiring the tangent and normal spaces, $\mathbf{T_i}$ and $\mathbf{N_i}$, for step i is crucial. This can be achieved by local SVD method [17], [18], which uses the leading eigenvectors of the $U = SVD(dist(\mathbf{x}_{i,l}{}_{l=1}^{K}))$ matrix to estimate the tangent and normal space, where $dist(\{\mathbf{x}_{i,l}\}_{l=1}^{K})$ is the local distance matrix induced by K-nearest neighbors of $\mathbf{x}_i$. With the current point $\mathbf{x}_i$, the initial step involves training the SINDy model to estimate the rate of change of $\Delta X_{\mathbf{T_i}}$ by solving the following optimization problem:

$$\min_{\Xi} \sum_{i=1}^{N} \left\| h(\mathbf{x}_i; \Xi) - \frac{\Delta \mathbf{x}_{\mathbf{T_i}}}{\Delta t} \right\|^2 + \lambda \|\Xi\|^2, \tag{2a}$$

$$\text{s.t.} \quad h(\mathbf{x}_i; \Xi) = \Xi \Theta(\mathbf{x}_i),\ \Xi \in R^{n \times k},\ \Theta \in R^{k \times 1}, \tag{2b}$$

where $\Theta(\mathbf{x}_i)$ is the library vector of the SINDy model, which includes all polynomials of $\mathbf{x}_i$ with order up to p. The parameter k denotes the number of terms in $\Theta(\mathbf{x}_i)$, Ξ denotes the coefficient matrix to be determined for the model, N denotes the total number of samples in the training set, and λ is the sparse norm coefficient.

C. Identification in the Normal Space Increment

The GMLS method is a versatile computational approach that enhances the standard least squares technique by considering weighted contributions from a moving neighborhood of data points to construct local approximations, thereby achieving higher accuracy in the representation of complex functions or data sets [16]. Specifically, denoting $\{\mathbf{x}_{i,\ell}\}_{\ell=1}^{K}$ as the set of K-nearest neighbors of $\mathbf{x}_i$, we approximate,

$$\Delta \mathbf{x}_{\mathbf{N_i}} \approx \mathbf{N}_i \hat{q}(\mathbf{x}_i),$$

where $\hat{q}$ is obtained by solving the following regression problem,

$$\hat{q} = \arg \min_{q \in \mathbb{P}_{\mathbf{x}_i}^{l,d}} \sum_{\ell=1}^{K} |\mathbf{N}_i^\top (\mathbf{x}_i - \mathbf{x}_{i,\ell}) - q(\mathbf{x}_{0,\ell})|^2, \tag{3}$$

over the following set of intrinsic local polynomials,

$$P_{\mathbf{x}_i}^{l,d} = \Big\{ q(\mathbf{x}) = \sum_{|\alpha| \le l} b_\alpha \prod_{j=1}^{d} \left(\mathbf{T}_i^\top (\mathbf{x} - \mathbf{x}_i) \right]^{\alpha_j} \Big\},$$

where $\alpha = (\alpha_1, \ldots, \alpha_d)$.

After the model preparation, it can be used to estimate the increment starting at $\hat{\mathbf{x}}_i$ following:

$$\hat{\mathbf{x}}_{i+1} = \hat{\mathbf{x}}_i + \hat{h}(\hat{\mathbf{x}}_i)\Delta t + \hat{\mathbf{N}}_i \hat{q}(\hat{\mathbf{x}}_i),$$

where the identifications of $\hat{h}$ in (2) and $\hat{q}$ in (3) require a local SVD method to construct tangent and normal vectors, $\{\hat{\mathbf{T}}_i, \hat{\mathbf{N}}_i\}$ of the new data point $\hat{\mathbf{x}}_i$.

IV. Numerical Examples

A. Test System and Training Data

A typical islanded microgrid system shown in Fig. 2 is used to test and validate the effectiveness of the presented method in modeling and predicting the system's transient dynamics. The loads in the system are modeled as constant impedance loads. More details of the test system can refer to [19].

The system has two specific control strategies corresponding to the grid-forming battery (V-f control) and grid-following wind turbine (P-Q control). Block diagrams explaining the details of the double-loop controller are given in [19], with the control parameters and initial state values given in Table I.

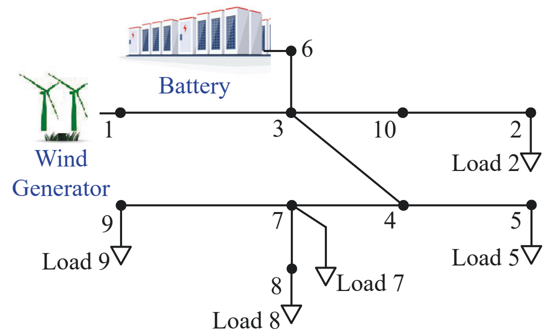

Fig. 2. Topology of the microgrid system used for test.

Table I Information of Model

$K_{P1,2}^{PLL}$	$K_{I1,2}^{Vreg}$	$K_{P1,2}^{Vreg}$	$K_{I1,2}^{Ireg}$	$K_{P1,2}^{Ireg}$	V_{ref}	ω_{ref}
10	15	0.8	35	0.05	1	0
P_{ref0}	Q_{ref0}	x_{01}	x_{02}	x_{03}	x_{04}	x_{05}
0.04	0	0	0	0.1498	0.8342	-0.1083
x_{06}	x_{07}	x_{08}	x_{09}	x_{010}	x_{011}	x_{012}
0.0245	0	0.0298	0.0408	0.7998	0	0.0067

A series of load adjustment values, ΔP, normally distributed within a range of -30% to $+30\%$ of rated value at a normal operation state, are applied to the active power P to simulate various operational scenarios of the system. To create a power transient, a load variation of 150% of their normal state is introduced into the system. For model training, 20 sample trajectories that capture these transients across different operational scenarios are generated using the model. These samples are recorded with a time window length of 0.6 seconds and a sampling rate of 1×10^{-3}. The key information of the simulation is summarized in Table II.

Table II Information of Simulation

time length ($t(s)$)	step size ($\delta t(s)$)	SINDy order p	GMLS order l	state space dim. n	tangent space dim. d
0.6	1×10^{-3}	2	3	12	1

The intrinsic dimension of the sample data can serve as a reference for the dimension d of the tangent space. However, fine-tuning may be necessary to optimize the performance.

B. Test Results

Additionally, 20 initial system operation states that are not part of the training trajectories are randomly chosen to evaluate the model's estimation performance. A representative result (+18% P case) of this estimation is depicted in Fig. 3. For display purposes, the voltage magnitude and angle at the inverter buses, along with the active and reactive power, are calculated from the original state variables due to their specific physical significance.

To demonstrate the significance of the geometric constraints, we compare the proposed approach (which we denote as the

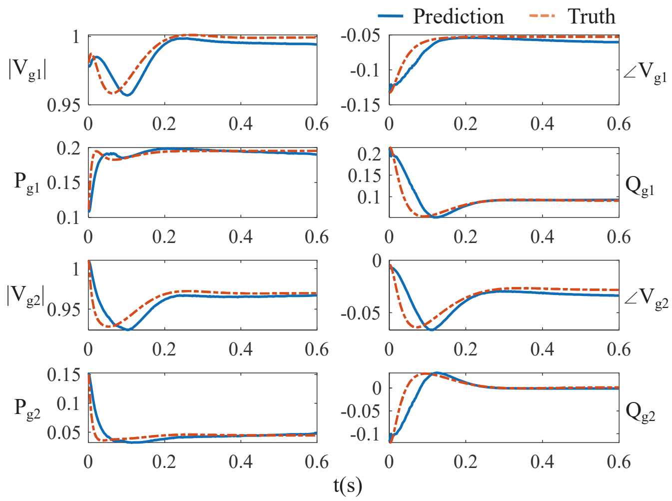

(a) Estimated results for key physical electrical amount on two generator buses.

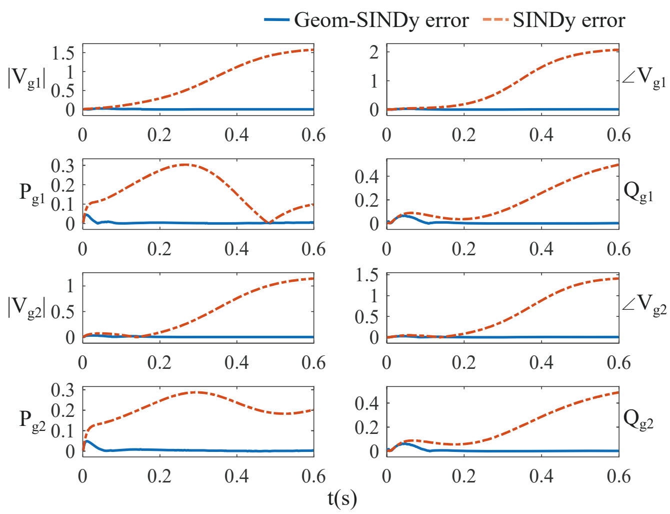

(b) Estimated absolute errors of Geom-SINDy and traditional SINDy method.

Fig. 3. Estimate results with initial states in the random testing set.

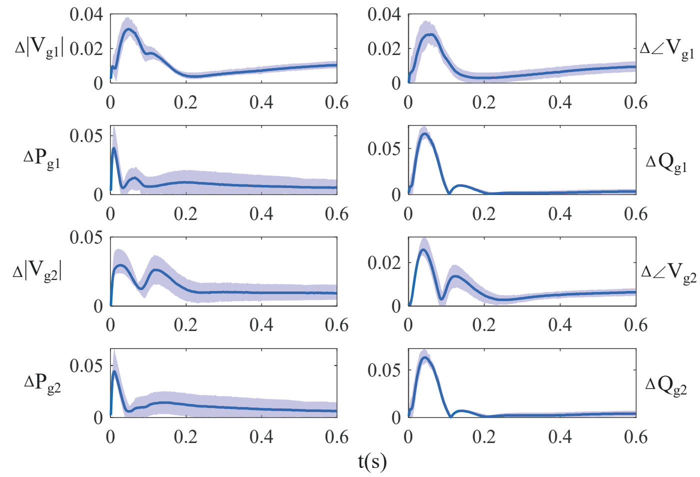

Fig. 4. Average absolute error with error band for all 20 tests of Geom-SINDy.

"Geom-SINDy") with the traditional SINDy model without geometric constraints, using a library of the same order-p. The key difference is that the library functions for the traditional SINDy is defined on the ambient coordinate, $\mathbf{x}$, in $\mathbb{R}^n$ without geometric constraints as proposed in Section III. The analysis of the results presented in Fig. 3 reveals that, although there are slight differences compared to the reference curve, the proposed model is essentially capable of capturing the dynamics associated with load variance disturbances, even with a limited set of training data. The traditional SINDy model has significantly worse performance compared to the proposed geom-SINDy method under the same condition as shown in Fig. 3b. This implies that the proposed method can improve the performance of the SINDy model with geometric-based candidate functions. This can help researchers to use less and simpler candidate function dictionary to realize the same performance.

The estimated average absolute error for all 20 tests are presented in Fig. 4, from which we can see that the errors across all estimated trajectories are limited and the average absolute error are less than 0.01 p.u., which means the estimated outcomes successfully capture the transients at different initial states. Essentially, this model offers a preliminary and rapid estimate of transients within the system.

V. Conclusions

A geometrically-constrained data-driven system identification method is introduced in the paper whose performance is less sensitive to the choice of candidate function dictionary, when compared to the conventional SINDy method. This method is used to model dynamic transients in the microgrid system caused by variations in load. The SINDy method and the GMLS algorithm are integrated to model the increments in the dynamic iteration by taking advantage of the geometric information inferred from the data manifold. The numerical results show that the proposed geometric constraints significantly improve the performance in capturing the transient dynamics based on limited training information and simple candidate functions. Further research will be conducted to improve model performance with an extension that includes control strategies.

Acknowledgment

This work is supported by the National Science Foundation under the award DMS-2229435.

Appendix

The differential equation sets (1a) summarize the model of transient dynamics. Define $V_{q,g1}(\theta_{g1}) = -V_i \cos\angle\alpha_i \sin\theta_{g1} + V_i \sin\angle\alpha_i \cos\theta_{g1}$, $I_{q,g1}(\theta_{g1}) = -I_i \cos\angle\alpha_i \sin\theta_{g1} +$

$I_i \sin\angle\alpha_i \cos\theta_{g1}$, and $I_{d,g1}(\theta_{g1}) = I_i \cos\angle\alpha_i \cos\theta_{g1} + I_i \sin\angle\alpha_i \sin\theta_{g1}$, similarly for generator 2, then the state equation can be listed as below.

$$\dot{x}_1 = V_{q,g1}(x_2) \tag{4a}$$
$$\dot{x}_2 = x_1 + K_{P1}^{PLL} V_{q,g1}(x_2) \tag{4b}$$
$$\dot{x}_3 = (V_{ref} - |V_{g1}|) K_{I1}^{Vreg} \tag{4c}$$
$$\dot{x}_4 = (x_3 + (V_{ref} - |V_{g1}|) K_{P1}^{Vreg} - I_{d,g1}) K_{I1}^{Ireg} \tag{4d}$$
$$\dot{x}_5 = (\omega_{ref} - \dot{x_2}) K_{I1}^{Vreg} \tag{4e}$$
$$\dot{x}_6 = (x_4 + (\omega_{ref} - \dot{x_2}) K_{P1}^{Vreg} - I_{q,g1}) K_{I1}^{Ireg} \tag{4f}$$
$$\dot{x}_7 = V_{q,g2}(x_8) \tag{4g}$$
$$\dot{x}_8 = x_7 + K_{P2}^{PLL} V_{q,g2}(x_8) \tag{4h}$$
$$\dot{x}_9 = (P_{ref} - P_{g2}) K_{I2}^{Vreg} \tag{4i}$$
$$\dot{x}_{10} = (x_9 + (P_{ref2} - P_{g2}) K_{P2}^{Vreg} - I_{d,g2}) K_{I2}^{Ireg} \tag{4j}$$
$$\dot{x}_{11} = (-Q_{ref} + Q_{g2}) K_{I2}^{Vreg} \tag{4k}$$
$$\dot{x}_{12} = (x_{10} + (-Q_{ref} + Q_{g2}) K_{P2}^{Vreg} - I_{q,g2}) K_{I2}^{Ireg} \tag{4l}$$

Then the inverter terminal voltage $\mathbf{V}_{inv\, g1,g2}$ can be obtained as follows,

$$E_{d,g1} = K_{P1}^{Ireg}(I_{d\,ref,g1} - I_{d,g1}) + x_4 \tag{5a}$$
$$E_{q,g1} = K_{P1}^{Ireg}(I_{q\,ref,g1} - I_{q,g1}) + x_6 \tag{5b}$$
$$E_{d,g2} = K_{P2}^{Ireg}(I_{d\,ref,g2} - I_{d,g2}) + x_{10} \tag{5c}$$
$$E_{q,g2} = K_{P2}^{Ireg}(I_{q\,ref,g2} - I_{q,g2}) + x_{12} \tag{5d}$$
$$\mathbf{E}_{\alpha,\beta\, g1} = T^{-1}(E_{d,g1}, E_{q,g1}) \tag{5e}$$
$$\mathbf{E}_{\alpha,\beta\, g2} = T^{-1}(E_{d,g2}, E_{q,g2}) \tag{5f}$$
$$\mathbf{V}_{\alpha,\beta\, g1} = 0.5\frac{\sqrt{3}}{\sqrt{2}} \mathbf{E}_{\alpha,\beta\, g1} V_{DC} \tag{5g}$$
$$\mathbf{V}_{\alpha,\beta\, g2} = 0.5\frac{\sqrt{3}}{\sqrt{2}} \mathbf{E}_{\alpha,\beta\, g2} V_{DC} \tag{5h}$$
$$\mathbf{V}_{inv\, g1} = V_{\alpha\, g1} + jV_{\beta\, g1} \tag{5i}$$
$$\mathbf{V}_{inv\, g2} = V_{\alpha\, g2} + jV_{\beta\, g2} \tag{5j}$$

REFERENCES

[1] V. K. Garg and S. Sharma, "Overview on microgrid system," in *2018 Fifth International Conference on Parallel, Distributed and Grid Computing (PDGC)*, 2018, pp. 694–699.

[2] N. M. Maletsie and S. Krishnamurthy, "Review of planning and optimization of the renewable-energy-based micro-grid for rural electrification," in *2024 32nd Southern African Universities Power Engineering Conference (SAUPEC)*, 2024, pp. 1–6.

[3] J. Zhang, C. Lu, and Y. Han, "Mimo identification of power system with low level probing tests: Applicability comparison of subspace methods," *IEEE Transactions on Power Systems*, vol. 28, no. 3, pp. 2907–2917, 2013.

[4] F. Al Hasnain, S. Kamalasadan, and M. Smith, "Electro-mechanical mode identification of a bess integrated grid system through subspace identification method," in *2022 IEEE Global Conference on Computing, Power and Communication Technologies (GlobConPT)*, 2022, pp. 1–6.

[5] A. Mohammadi, H. Khaloozadeh, and R. Amjadifard, "Power system monitoring using subspace identification," in *The 2nd International Conference on Control, Instrumentation and Automation*, 2011, pp. 19–24.

[6] X. Jiang, Y. Li, and D. Huang, "Data-driven modeling and prediction of transient dynamics of microgrids through dynamic mode decomposition with control," in *2024 IEEE Power Energy Society Innovative Smart Grid Technologies Conference (ISGT)*, 2024, pp. 1–5.

[7] K. Aleikish and T. Øyvang, "Real-time identification of electromechanical oscillations via deep learning enhanced dynamic mode decomposition," in *2023 IEEE Power Energy Society General Meeting (PESGM)*, 2023, pp. 1–5.

[8] S. Sinha, S. P. Nandanoori, and E. Yeung, "Data driven online learning of power system dynamics," in *2020 IEEE Power Energy Society General Meeting (PESGM)*, 2020, pp. 1–5.

[9] X. Liu, L. Zheng, Z. Wang, and Y. Sun, "State prediction of small signal synchronous stability of converter interfaced generation system based on koopman operator and time delay embedding," in *2023 IEEE Sustainable Power and Energy Conference (iSPEC)*, 2023, pp. 1–6.

[10] B. Liao and R. Ma, "Power system load dynamic characteristics identification based on elman neural network," in *2011 International Conference on Electrical and Control Engineering*, 2011, pp. 4010–4013.

[11] Y. Qiu, Y. Wang, Y. Tian, and Z. Chen, "Artificial neural network-based intelligent grid impedance identification method for grid-connected inverter," in *2022 International Power Electronics Conference (IPEC-Himeji 2022- ECCE Asia)*, 2022, pp. 992–997.

[12] M. G. Jahromi, S. D. Mitchell, G. Mirzaeva, and D. Gay, "A new method for power system load modeling using a nonlinear system identification estimator," *IEEE Transactions on Industry Applications*, vol. 52, no. 4, pp. 3535–3542, 2016.

[13] J. L. P. Steven L. Brunton and J. N. Kutz, "Discovering governing equations from data by sparse identification of nonlinear dynamical systems," *PNAS APPLIED MATHEMATICS*, vol. 113, no. 15, pp. 3932–3937, 2016.

[14] A. Hamid, D. Rafiq, S. A. Nahvi, and M. A. Bazaz, "Power grid parameter estimation using sparse identification of nonlinear dynamics," in *2022 International Conference on Intelligent Controller and Computing for Smart Power (ICICCSP)*, 2022, pp. 1–6.

[15] Y. Cai, X. Wang, G. Joós, and I. Kamwa, "An online data-driven method to locate forced oscillation sources from power plants based on sparse identification of nonlinear dynamics (sindy)," *IEEE Transactions on Power Systems*, vol. 38, no. 3, pp. 2085–2099, 2023.

[16] D. Mirzaei, R. Schaback, and M. Dehghan, "On generalized moving least squares and diffuse derivatives," *IMA Journal of Numerical Analysis*, vol. 32, no. 3, pp. 983–1000, 2012.

[17] D. L. Donoho and C. Grimes, "Hessian eigenmaps: Locally linear embedding techniques for high-dimensional data," *Proceedings of the National Academy of Sciences*, vol. 100, no. 10, pp. 5591–5596, 2003.

[18] H. Tyagi, E. Vural, and P. Frossard, "Tangent space estimation for smooth embeddings of Riemannian manifolds," *Information and Inference: A Journal of the IMA*, vol. 2, no. 1, pp. 69–114, 2013.

[19] A. Nandakumar, Y. Li, H. Zheng, J. Zhao, D. Zhao, Y. Zhang, T. Hong, and B. Chen, "Data-driven modeling of microgrid transient dynamics through modularized sparse identification," *IEEE Transactions on Sustainable Energy*, 2023.